

Supporting Information

CFA-15 – a perfluorinated metal-organic framework with linear 1-D Cu^{II}-chains containing accessible unsaturated, reactive metal centres

J. Fritzsche,^a R. Ettlinger,^a M. Grzywa,^a S. G. Jantz,^a A. Kalytta-Mewes,^a H. Bunzen,^a H. A. Höppe^a and D. Volkmer ^{*a}

^a Institute of Physics, Chair of Solid State and Materials Chemistry, University of Augsburg, Universitätsstrasse 1, 86159 Augsburg, Germany

Contents:

1.	IR spectra	S2
2.	Gas sorption measurements	S6
3.	Crystallographic data	S11
4.	XRPD pattern	S22
5.	Rietveld refinement plots	S23
6.	DFT calculations	S

* Corresponding author. Fax: +49 (0)821 598–5955; Tel: +49 (0)821 598–3006; E-mail:
dirk.volkmmer@physik.uni-augsburg.de

1. IR- Spectra

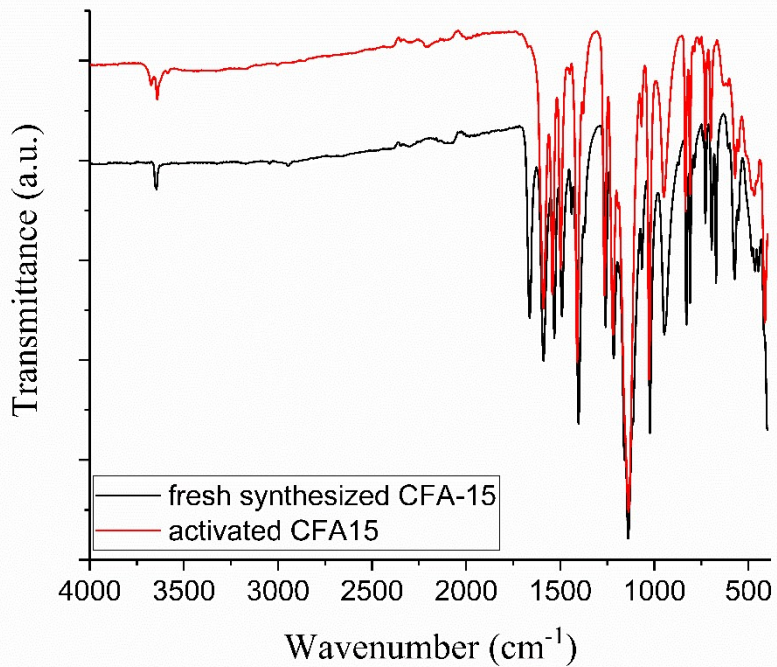


Fig. S1 Full-range IR spectra of fresh synthesized **CFA-15** (black curve) and activated **CFA-15** (red curve).

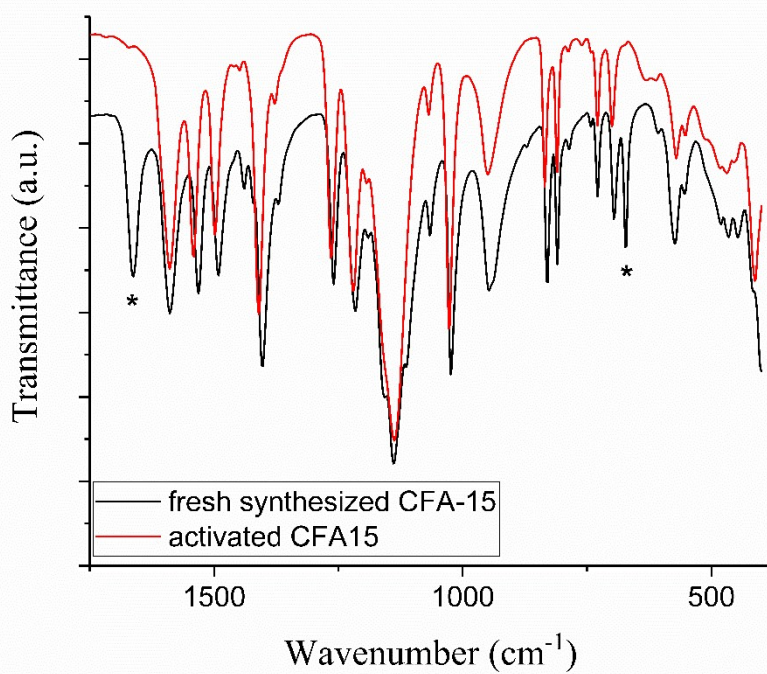


Fig. S2 IR spectra in the range of 1750-400 cm⁻¹ of fresh synthesized **CFA-15** (black curve) and activated **CFA-15** (red curve) (* - a characteristic band of coordinated DMF molecules).

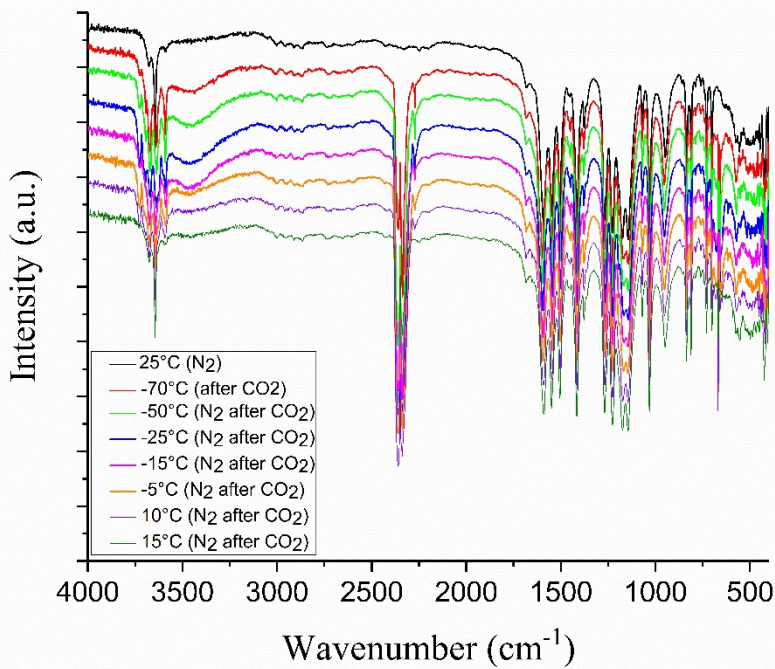


Fig. S3 Full-range in situ DRIFT spectra of **CFA-15** upon cooling from room temperature to -70 °C under CO₂ and subsequent heating from -70 °C to 15 °C under N₂. The black curve shows the sample under N₂ at room temperature without any CO₂ contact.

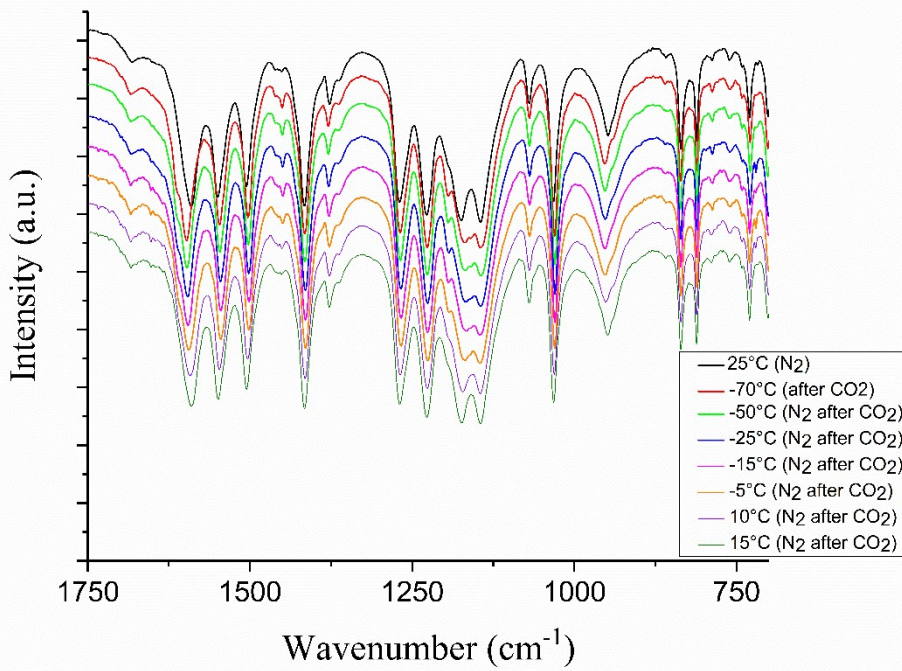


Fig. S4 In situ DRIFT spectra of **CFA-15** in the range of 700 – 1750 cm^{-1} upon cooling from room temperature to -70 °C under CO₂ and subsequent heating from -70 °C to 15 °C under N₂. The black curve shows the sample under N₂ at room temperature without any CO₂ contact.

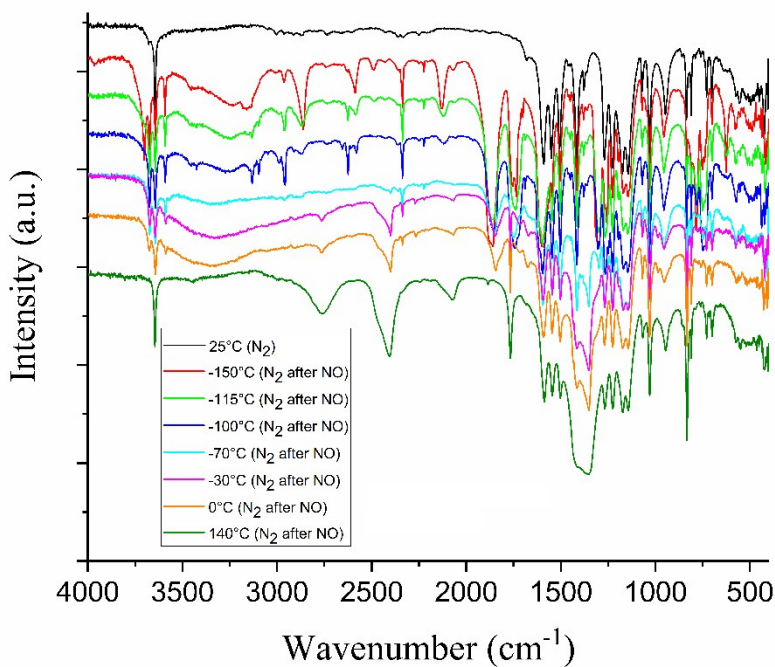


Fig. S5 Full-range in situ DRIFT spectra of **CFA-15** upon cooling from room temperature to -150 °C under NO and subsequent heating from -150 °C to 140 °C under N₂. The black curve shows the sample under N₂ at room temperature without any NO contact.

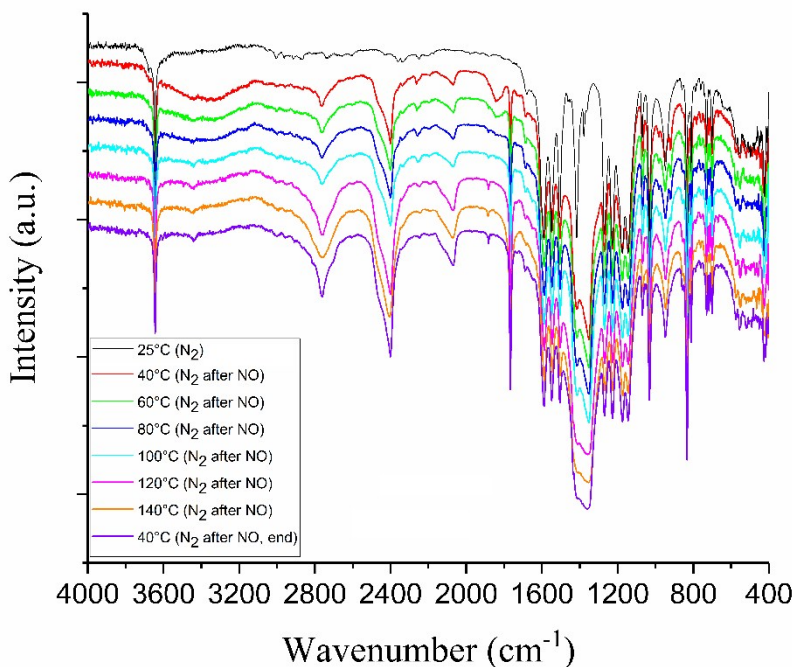


Fig. S6 Full-range in situ DRIFT spectra of **CFA-15** upon subsequent heating under N₂ after treatment with NO. The black curve shows the sample under N₂ at room temperature without any NO contact.



Fig. S7 Colour change of activated CFA-15 after treatment with NO.

2. Gas sorption measurements

The isosteric heats of adsorption were calculated from the measured isotherms (Figs. S3-6) using the Clausius-Clapeyron equation (I). The slopes of linear plots $\ln P$ versus $1/RT$ for different loadings (Fig. S7-10) give the adsorption enthalpies, according to the equation (II).

$$Q_{st} = -R \left(\frac{\partial(\ln P)}{\partial(1/T)} \right)_{\theta} \quad (\text{I}), \Theta - \text{surface coverage}$$

$$\ln P = -\frac{Q_{st}}{R} \left(\frac{1}{T} \right) + C \quad (\text{II}), C - \text{integration constant}$$

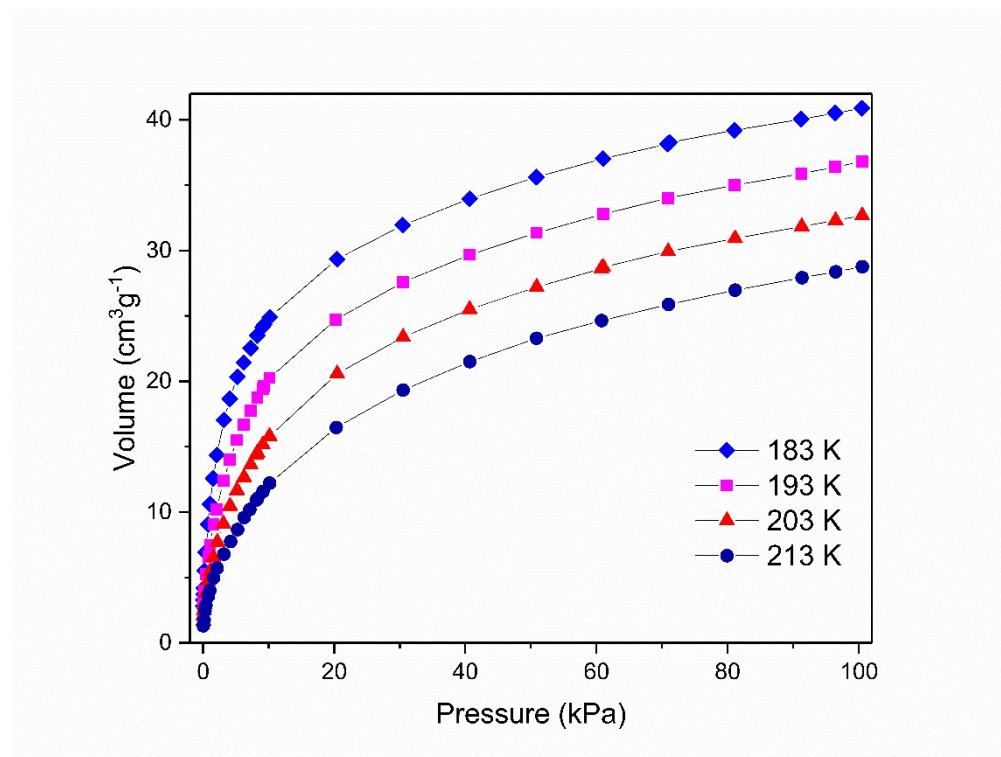


Fig. S8 CO adsorption isotherms of **CFA-15** at different temperatures.

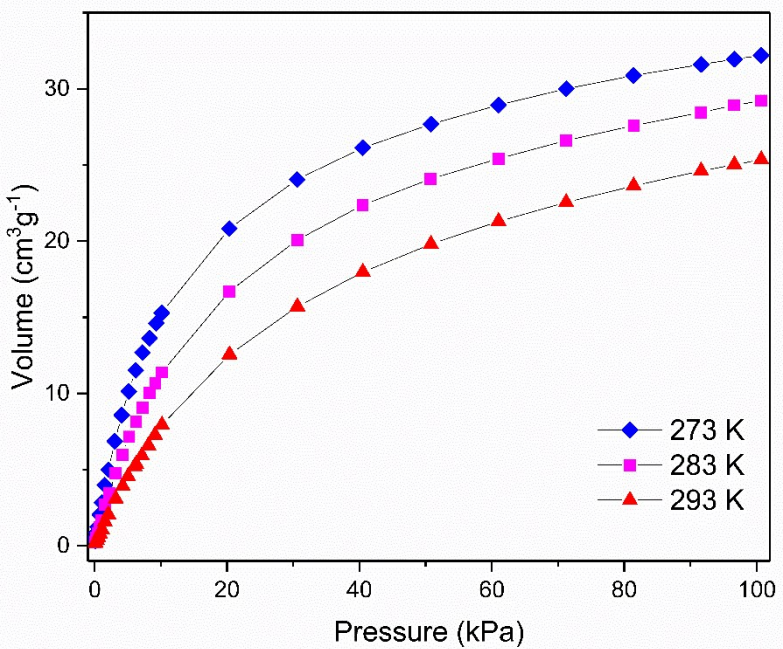


Fig. S9 CO₂ adsorption isotherms of **CFA-15** at different temperatures.

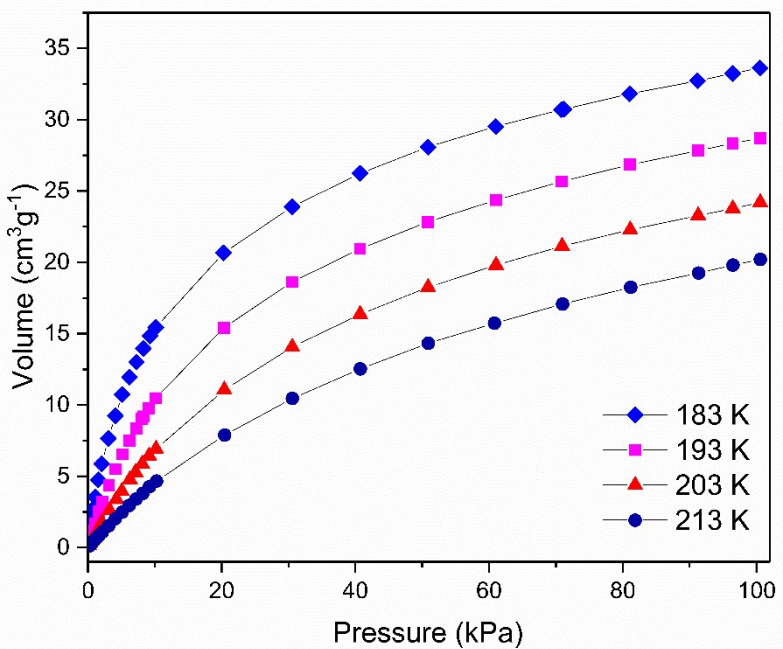


Fig. S10 O₂ adsorption isotherms of **CFA-15** at different temperatures.

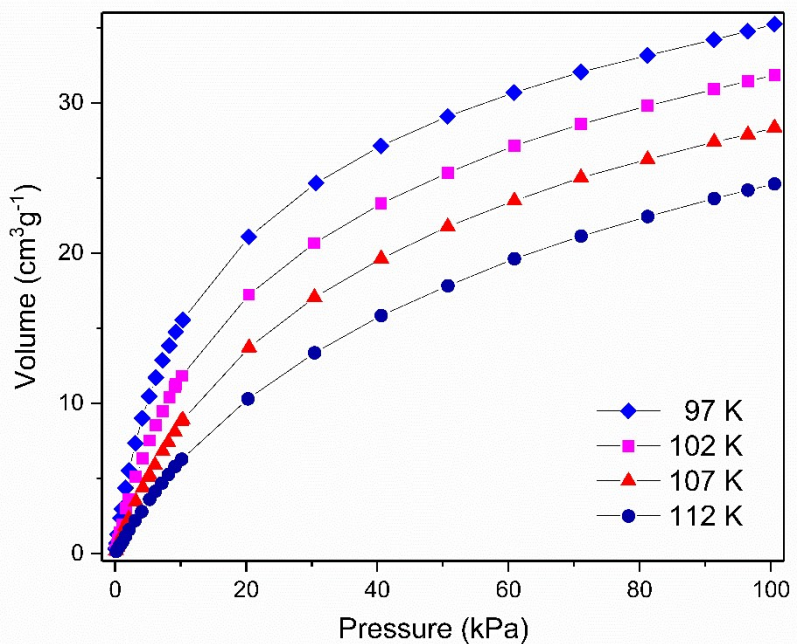


Fig. S11 H₂ adsorption isotherms of **CFA-15** at different temperatures.

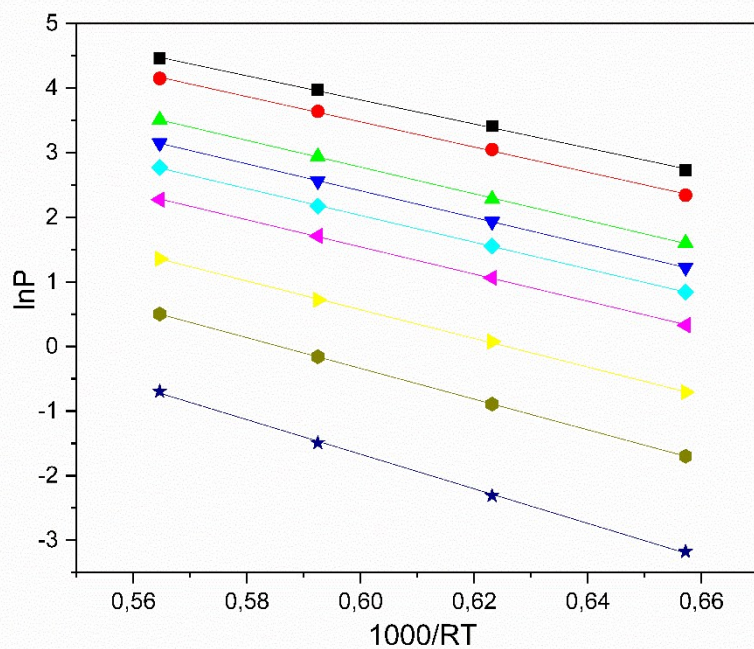


Fig. S12 lnP versus 1000/RT plots for different loadings of CO adsorption on **CFA-15**.

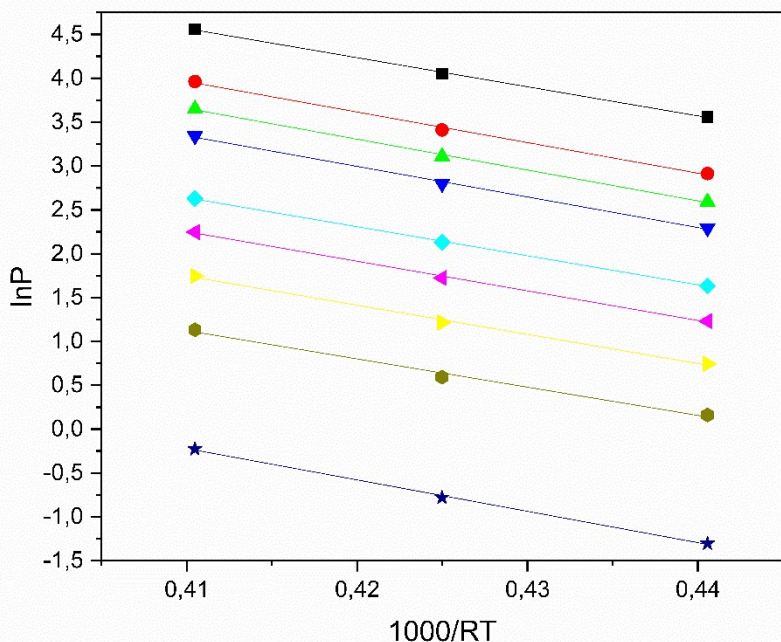


Fig. S13 $\ln P$ versus $1000/RT$ plots for different loadings of CO_2 adsorption on **CFA-15**.

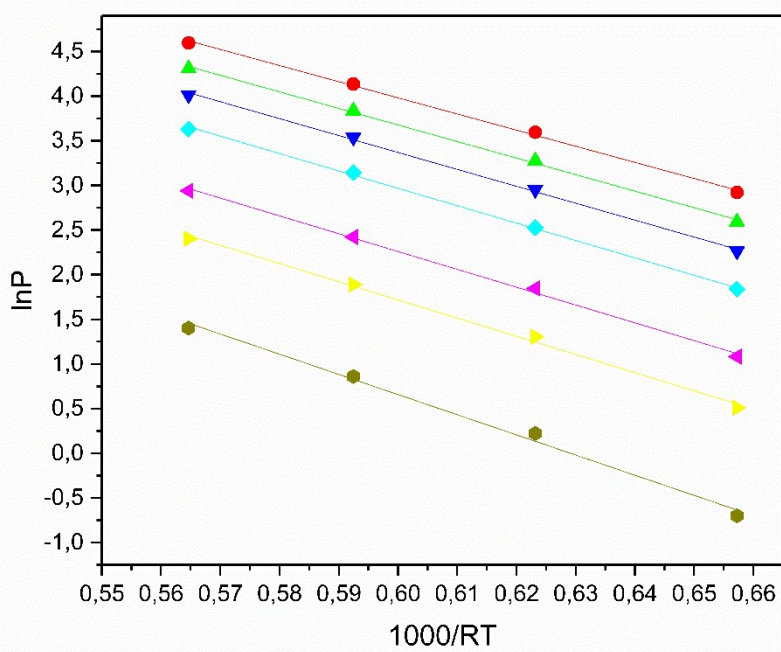


Fig. S14 $\ln P$ versus $1000/RT$ plots for different loadings of O_2 adsorption on **CFA-15**.

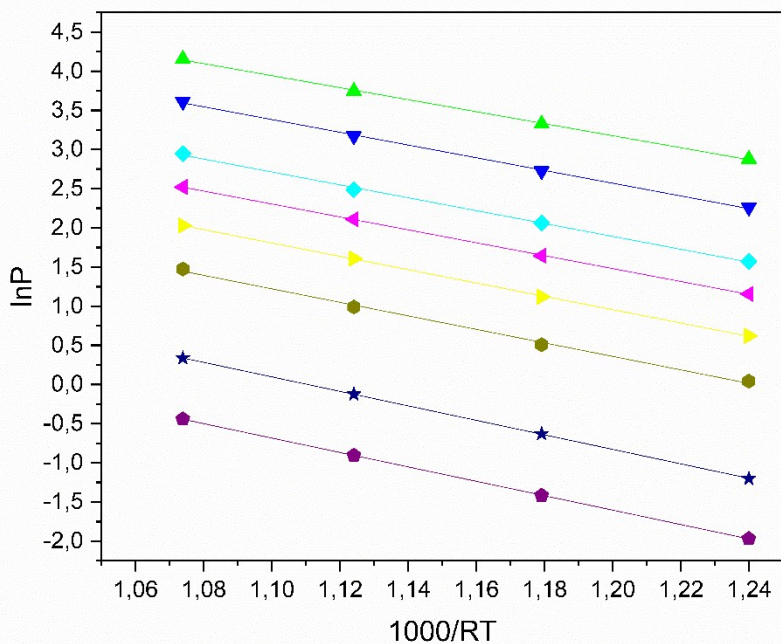


Fig. S15 $\ln P$ versus $1000/RT$ plots for different loadings of H_2 adsorption on **CFA-15**.

3. Crystallographic data

Single Crystal Structure Analysis of CFA-15:

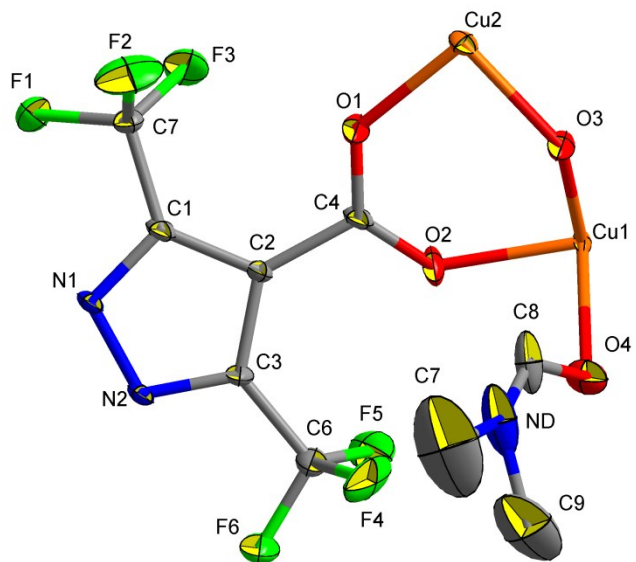


Fig. S16 ORTEP-style plot of the asymmetric unit of **CFA-15**. Thermal ellipsoids probability: 50 %. Hydrogen atoms have been omitted for clarity.

Table S1. Atomic coordinates ($\times 10^4$) and equivalent isotropic displacement parameters ($\text{\AA}^2 \times 10^3$) for **CFA-15**. U(eq) is defined as one third of the trace of the orthogonalized U_{ij} tensor.

	x	y	z	U(eq)
Cu1	4775.1(8)	7026.0(12)	6592.3(12)	10.8(3)
Cu2	5000	5739.2(17)	10000	15.1(4)
F2	2344(8)	3322(12)	10031(10)	54(3)
O2	3528(5)	6003(9)	6433(9)	27.3(19)
F5	2121(7)	5765(10)	3600(8)	53(2)
N2	1071(6)	3227(9)	5109(9)	12.6(16)
F6	1334(5)	3924(9)	2576(7)	36.3(19)
N1	965(6)	3166(9)	6520(9)	13.0(16)
F3	1975(6)	5480(9)	9522(9)	45(2)
O3	5470(5)	6018(9)	8382(8)	23.6(19)
F4	2884(6)	3807(12)	3758(10)	55(3)
O1	3656(6)	5268(10)	8738(8)	31(2)
C1	1698(7)	3938(11)	7459(10)	13.0(19)
O4	5000	5368(11)	5000	25(2)
F1	818(6)	3966(10)	9161(9)	47(2)
C2	2301(9)	4531(13)	6695(13)	14.0(19)
C6	2063(8)	4395(13)	3799(12)	24(2)
C4	3238(8)	5340(11)	7343(12)	18(2)
C5	1720(8)	4170(12)	9050(11)	21(2)
C3	1839(7)	4056(11)	5210(10)	14.4(19)
ND	5000	2973(16)	5000	41(4)
C0AA	5012(19)	4180(20)	5540(30)	31(5)
C1AA	4880(30)	2920(30)	3220(40)	62(9)
C2AA	5100(30)	1630(30)	5600(40)	65(11)

Table S2. Bond lengths [Å] and angles [°] for **CFA-15**.

Cu(1)-O(2)	1.991(7)	O(2)-Cu(1)-N(2) ¹	86.1(3)
Cu(1)-N(2) ¹	2.003(8)	O(2)-Cu(1)-N(1) ²	173.5(3)
Cu(1)-N(1) ²	2.037(8)	O(2)-Cu(1)-O(4)	86.3(3)
Cu(1)-O(3)	1.897(7)	N(2) ¹ -Cu(1)-N(1) ²	87.6(3)
Cu(1)-O(4)	2.266(7)	N(2) ¹ -Cu(1)-O(4)	92.9(3)
Cu(2)-O(3)	1.876(7)	N(1) ² -Cu(1)-O(4)	92.3(3)
Cu(2)-O(3) ³	1.876(7)	O(3)-Cu(1)-O(2)	90.5(3)
Cu(2)-O(1)	1.939(7)	O(3)-Cu(1)-N(2) ¹	171.3(4)
Cu(2)-O(1) ³	1.939(7)	O(3)-Cu(1)-N(1) ²	95.9(3)
F(2)-C(5)	1.318(14)	O(3)-Cu(1)-O(4)	94.9(3)
O(2)-C(4)	1.240(13)	O(3)-Cu(2)-O(3) ³	163.8(6)
F(5)-C(6)	1.319(15)	O(3) ³ -Cu(2)-O(1)	88.6(3)
N(2)-N(1)	1.384(11)	O(3)-Cu(2)-O(1)	95.1(3)
N(2)-C(3)	1.328(12)	O(3)-Cu(2)-O(1) ³	88.6(3)
F(6)-C(6)	1.341(12)	O(3) ³ -Cu(2)-O(1) ³	95.1(3)
N(1)-C(1)	1.338(12)	O(1)-Cu(2)-O(1) ³	153.3(6)
F(3)-C(5)	1.329(13)	C(4)-O(2)-Cu(1)	134.0(7)
F(4)-C(6)	1.311(14)	N(1)-N(2)-Cu(1) ⁴	120.5(6)
O(1)-C(4)	1.244(13)	C(3)-N(2)-Cu(1) ⁴	131.0(7)
C(1)-C(2)	1.410(15)	C(3)-N(2)-N(1)	108.2(8)
C(1)-C(5)	1.500(14)	N(2)-N(1)-Cu(1) ⁵	114.6(6)
O(4)-C(0AA)	1.23(2)	C(1)-N(1)-Cu(1) ⁵	138.3(7)
F(1)-C(5)	1.343(13)	C(1)-N(1)-N(2)	107.0(8)
C(2)-C(4)	1.485(15)	Cu(2)-O(3)-Cu(1)	124.3(4)
C(2)-C(3)	1.401(14)	C(4)-O(1)-Cu(2)	131.0(7)
C(6)-C(3)	1.499(14)	N(1)-C(1)-C(2)	111.2(9)
ND-C(0AA)	1.25(3)	N(1)-C(1)-C(5)	119.0(9)
ND-C(1AA)	1.62(4)	C(2)-C(1)-C(5)	129.5(9)
ND-C(2AA)	1.38(3)	Cu(1)-O(4)-Cu(1) ⁶	92.1(4)
		C(0AA)-O(4)-Cu(1) ⁶	156.7(12)
		C(0AA)-O(4)-Cu(1)	110.6(12)
		C(1)-C(2)-C(4)	128.3(10)
		C(3)-C(2)-C(1)	102.3(9)
		C(3)-C(2)-C(4)	129.1(10)
		F(5)-C(6)-F(6)	106.0(9)
		F(5)-C(6)-C(3)	112.2(10)
		F(6)-C(6)-C(3)	110.4(9)

F(4)-C(6)-F(5)	108.4(10)
F(4)-C(6)-F(6)	106.2(10)
F(4)-C(6)-C(3)	113.2(10)
O(2)-C(4)-O(1)	126.8(10)
O(2)-C(4)-C(2)	116.5(9)
O(1)-C(4)-C(2)	116.7(10)
F(2)-C(5)-F(3)	107.0(9)
F(2)-C(5)-C(1)	112.8(10)
F(2)-C(5)-F(1)	107.5(10)
F(3)-C(5)-C(1)	112.4(9)
F(3)-C(5)-F(1)	105.7(10)
F(1)-C(5)-C(1)	111.0(9)
N(2)-C(3)-C(2)	111.2(9)
N(2)-C(3)-C(6)	118.9(9)
C(2)-C(3)-C(6)	129.9(9)
C(0AA)-ND-C(1AA)	115.3(18)
C(0AA)-ND-C(2AA)	134.1(19)
C(2AA)-ND-C(1AA)	111(2)
O(4)-C(0AA)-ND	133(2)

Symmetry transformations used to generate equivalent atoms:

¹1/2-X,1/2+Y,1-Z; ²1/2+X,1/2+Y,+Z; ³1-X,+Y,2-Z; ⁴1/2-X,-1/2+Y,1-Z; ⁵-1/2+X,-1/2+Y,+Z; ⁶1-X,+Y,1-Z

Table S3. Anisotropic displacement parameters ($\text{\AA}^2 \times 10^3$) for **CFA-15**. The anisotropic displacement factor exponent takes the form: $-2\pi^2 [h^2 a^* U_{11} + \dots + 2 h k a^* b^* U_{12}]$

	U ₁₁	U ₂₂	U ₃₃	U ₂₃	U ₁₃	U ₁₂
Cu1	6.7(5)	15.0(6)	8.3(5)	5.1(6)	-0.9(4)	-3.0(5)
Cu2	10.7(9)	19.8(10)	11.5(9)	0	-0.7(7)	0
F2	66(6)	71(6)	18(4)	17(4)	4(4)	20(5)
O2	15(4)	38(5)	24(4)	9(4)	1(3)	-15(3)
F5	82(6)	50(5)	24(4)	9(4)	13(4)	-30(5)
N2	9(4)	15(4)	12(4)	0(3)	1(3)	-1(3)
F6	32(4)	59(5)	14(3)	-2(3)	3(3)	-16(4)
N1	12(4)	14(4)	9(4)	1(3)	-1(3)	-2(3)
F3	64(5)	42(4)	39(4)	-27(4)	30(4)	-23(4)
O3	13(4)	42(5)	13(4)	17(4)	0(3)	-1(3)
F4	26(4)	113(8)	35(5)	1(5)	22(4)	5(5)
O1	18(4)	58(6)	11(3)	-3(4)	-3(3)	-21(4)
C1	13(4)	16(5)	7(4)	0(3)	-1(3)	-2(3)
O4	35(6)	15(5)	23(5)	0	6(5)	0
F1	38(4)	80(6)	33(4)	-23(4)	25(3)	-26(4)
C2	15(4)	16(5)	9(4)	-1(4)	2(3)	-5(3)
C6	19(5)	42(6)	10(4)	2(5)	2(4)	-11(4)
C4	13(5)	20(5)	16(4)	-2(4)	2(4)	-4(4)
C5	24(5)	29(5)	10(4)	0(4)	5(4)	-8(4)
C3	13(4)	19(5)	9(4)	1(4)	2(3)	-2(4)
ND	23(8)	19(6)	81(11)	0	17(8)	0
C0AA	27(11)	20(6)	46(13)	9(6)	13(12)	2(8)
C1AA	80(30)	24(15)	73(13)	-20(12)	20(17)	-9(15)
C2AA	80(30)	21(10)	100(30)	11(12)	30(30)	8(13)

Single Crystal Structure Analysis of 3,5-bis(trifluoromethyl)pyrazole-4-carboxylic acid ($\text{H}_2\text{-tfpc}$) ($\text{C}_6\text{H}_2\text{F}_6\text{N}_2\text{O}_2$):

$\text{H}_2\text{-tfpc}$ crystallizes in the orthorhombic crystal system within the space group $Cmc2_1$ (no. 36). The asymmetric unit consists of two nitrogen, six carbon, six fluoride, two oxygen and two hydrogen atoms accounting for one $\text{H}_2\text{-tfpc}$ ligand. The two nitrogen atoms and three carbon atoms form a five-membered ring with two CF_3 -groups and one COOH group attached to the ring-building carbon atoms. An ORTEP-style plot of $\text{H}_2\text{-tfpc}$ is shown in Fig. S12.

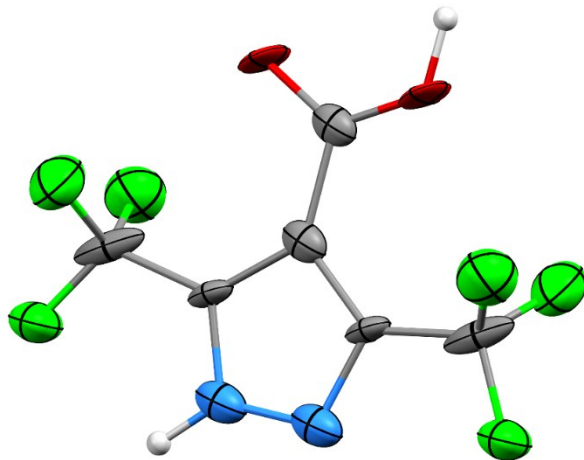


Fig. S17 ORTEP-style plot of $\text{H}_2\text{-tfpc}$. Thermal ellipsoids probability: 50 %. red: Oxygen; green: fluorine; grey: carbon; blue: nitrogen; white: hydrogen.

The $\text{H}_2\text{-tfpc}$ molecules form layers orthogonal to the a -axis with only the F32 and F52 atoms not lying in the bc -mirror plane. There are formed weak hydrogen bonds between the COOH and the NNH groups. A list of the hydrogen bonds for $\text{H}_2\text{-tfpc}$ is presented in Table S5. The packing plots of $\text{H}_2\text{-tfpc}$ along each direction are shown in Fig. S13. A list of the bond lengths and angles for $\text{H}_2\text{-tfpc}$ is presented in Table S4. Table S6 shows the anisotropic displacement parameters for $\text{H}_2\text{-tfpc}$ and Table S7 displays the atomic coordinates.

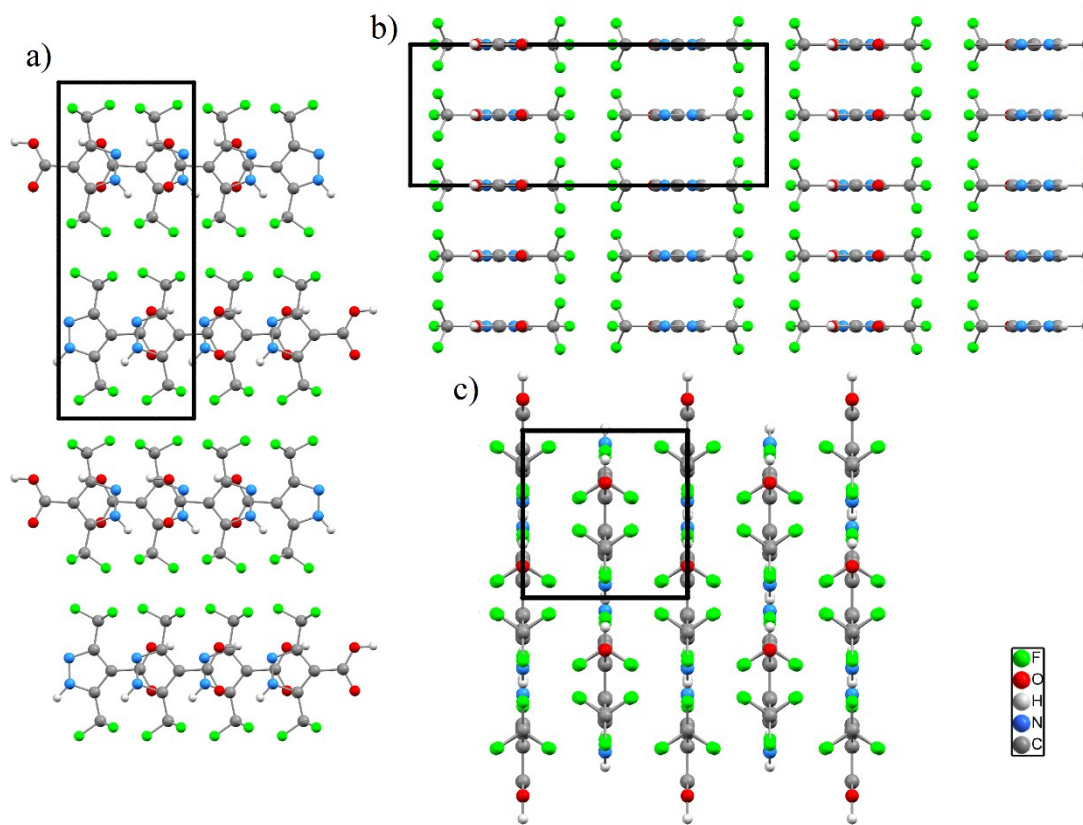


Fig. S18 Packing diagram of $\text{H}_2\text{-tfpc}$: a) view along a -axis; b) view along b -axis; c) view along c -axis.

Table S4 Bond lengths [\AA] and angles [$^\circ$] for $\text{H}_2\text{-tfpc}$.

F(51)-C(51)	1.3293(17)	C (41)-O (1)-H (1)	122.0 (14)
F(31)-C(31)	1.3294(17)	N (2)-N (1)-C (5)	110.3 (4)
F(52)-C(51)	1.3294(15)	N (2)-N (1)-H (2)	136.5 (16)
F(32)-C(31)	1.3294(15)	C (5)-N (1)-H (2)	113.2 (17)
O(1)-C(41)	1.256(11)	N (1)-N (2)-C (3)	106.7 (3)
O(1)-H(1)	0.960(14)	O (1)-C (41)-O (2)	123.5 (11)
O(2)-C(41)	1.256(11)	O (1)-C (41)-C (4)	121.1 (9)
N(1)-N(2)	1.328(9)	O (2)-C (41)-C (4)	115.4 (9)
N(1)-C(5)	1.332(3)	C (41)-C (4)-C (5)	131.2 (6)
N(1)-H(2)	0.960(13)	C (41)-C (4)-C (3)	126.3 (5)
N(2)-C(3)	1.332(3)	C (5)-C (4)-C (3)	102.6 (8)
C(41)-O(1)	1.256(11)	N (1)-C (5)-C (4)	109.1 (5)
C(41)-O(2)	1.256(11)	N (1)-C (5)-C (51)	120.4 (3)
C(41)-C(4)	1.462(18)	C (4)-C (5)-C (51)	130.5 (4)
C(4)-C(5)	1.393(8)	N (2)-C (3)-C (4)	111.3 (5)
C(4)-C(3)	1.393(8)	N (2)-C (3)-C (31)	116.7 (3)
C(4)-C(41)	1.462(18)	C (4)-C (3)-C (31)	132.0 (4)
C(5)-C(4)	1.393(8)	F (51)-C (51)-F (52)	105.09 (19)
C(5)-C(51)	1.495(2)	F (51)-C (51)-C (5)	113.66 (19)
C(3)-C(4)	1.393(8)	F (51)-C (51)-F (52)	105.09 (19)
C(3)-C(31)	1.495(2)	F (52)-C (51)-C (5)	109.9 (2)
C(51)-F(52)	1.3294(15)	F (52)-C (51)-F (52)	113.2 (3)
C(31)-F(32)	1.3294(15)	C (5)-C (51)-F (52)	109.9 (2)
		F (31)-C (31)-F (32)	109.42 (18)
		F (31)-C (31)-C (3)	109.2 (2)
		F (31)-C (31)-F (32)	109.42 (18)
		F (32)-C (31)-C (3)	114.02 (18)
		F (32)-C (31)-F (32)	100.4 (2)
		C (3)-C (31)-F (32)	114.02 (18)

Table S5 Hydrogen bonds for $\text{H}_2\text{-tfpc}$.

Donor---Hydrogen...Acceptor	Don--Hyd [\AA]	Hyd--Acc [\AA]	Don--Acc [\AA]	D--H----A
O1---H1...N2	0.960(14)	1.853(17)	2.761(10)	156.6(16) $^\circ$
N1---H2...O2	0.960(13)	2.12(3)	2.748(11)	122.1(18) $^\circ$

Table S6. Anisotropic displacement parameters ($\text{\AA}^2 \times 10^3$) for H₂-tfpc. The anisotropic displacement factor exponent takes the form: $-2\pi^2 [h^2 a^{*2} U_{11} + \dots + 2 h k a^{*} b^{*} U_{12}]$

	U ₁₁	U ₂₂	U ₃₃	U ₂₃	U ₁₃	U ₁₂
F(51)	0.071(4)	0.024(3)	0.042(3)	-0.001(4)	0	0
F(31)	0.071(4)	0.024(3)	0.042(3)	-0.001(4)	0	0
F(52)	0.064(3)	0.052(2)	0.048(2)	-0.007(4)	0.009(2)	0.011(5)
F(32)	0.064(3)	0.052(2)	0.048(2)	-0.007(4)	0.009(2)	0.011(5)
O(1)	0.070(5)	0.018(3)	0.029(4)	0.018(5)	0	0
O(2)	0.070(5)	0.018(3)	0.029(4)	0.018(5)	0	0
N(1)	0.028(4)	0.024(4)	0.049(4)	-0.006(9)	0	0
N(2)	0.028(4)	0.024(4)	0.049(4)	-0.006(9)	0	0
C(41)	0.018(5)	0.024(4)	0.038(5)	0.006(10)	0	0
C(4)	0.018(5)	0.024(4)	0.038(5)	0.006(10)	0	0
C(5)	0.021(5)	0.015(5)	0.030(6)	0.012(8)	0	0
C(3)	0.021(5)	0.015(5)	0.030(6)	0.012(8)	0	0
C(51)	0.012(5)	0.033(6)	0.077(7)	0.036(10)	0	0
C(31)	0.012(5)	0.033(6)	0.077(7)	0.036(10)	0	0

Table S7. Atomic coordinates for H₂-tfpc.

	x	y	z	U _{iso}
F51	0	0.3485(3)	0.44545(16)	0.0458(17)
F31	0	0.3781(3)	0.0667(2)	0.0458(17)
F52	0.3365(2)	0.4035(4)	0.9198(2)	0.0547(13)
F32	0.6505(3)	0.3980(4)	0.5771(2)	0.0547(13)
O1	0	0.8148(14)	0.1818(6)	0.039(2)
O2	0	0.8122(15)	0.3107(5)	0.039(2)
N1	0	0.4175(4)	0.2904(4)	0.033(2)
N2	0	0.4226(4)	0.2131(4)	0.033(2)
C41	0	0.1004(18)	0.7465(6)	0.026(2)
C4	0	0.8890(18)	0.75139(6)	0.026(2)
C5	0	0.2349(3)	0.31545(8)	0.022(2)
C3	0	0.2394(3)	0.18879(8)	0.022(2)
C51	0	0.1914(2)	0.40074(9)	0.041(3)
C31	0	0.2076(2)	0.10268(9)	0.041(3)
H1	0	0.676(2)	0.1777(10)	0,05
H2	0	0.511(4)	0.3320(9)	0,05

Crystal data of activated CFA-15:

Table S8 Atomic coordinates of activated **CFA-15** (fractional).

no	atom	xf	yf	zf	sigxf	sigyf	sigzf
1	Cu1	0.519108	0.692304	0.833082	0.001000	0.000100	0.002000
2	Cu2	0.500000	0.553903	0.500000	0.000000	0.000100	0.000000
3	F2	0.234086	0.320457	0.499525	0.002000	0.000100	0.000300
4	F3	0.186398	0.546821	0.458000	0.002000	0.000100	0.001000
5	F5	0.232059	0.571269	-0.180372	0.002000	0.001000	0.004000
6	F4	0.291986	0.372121	-0.134206	0.003000	0.000500	0.005000
7	O2	0.363162	0.583462	0.148622	0.003000	0.001000	0.005000
8	O3	0.452451	0.574429	0.666742	0.000100	0.000100	0.000100
9	F6	0.143061	0.383821	-0.245337	0.000900	0.000100	0.000200
10	F1	0.080562	0.384921	0.429854	0.001000	0.000000	0.000400
11	N2	0.105224	0.318037	0.011506	0.000100	0.000000	0.000100
12	O1	0.361705	0.521428	0.376300	0.000900	0.000000	0.000000
13	N1	0.094325	0.309137	0.149899	0.000100	0.000400	0.000100
14	C1	0.166061	0.386350	0.248725	0.000800	0.000100	0.000900
15	C6	0.197844	0.454628	-0.119852	0.000100	0.000100	0.000900
16	C4	0.324121	0.523150	0.235400	0.000100	0.000100	0.000100
17	C2	0.229055	0.444158	0.172908	0.000100	0.000200	0.000100
18	C3	0.182900	0.400750	0.021600	0.002000	0.001000	0.001000
19	C5	0.167848	0.410050	0.408658	0.000700	0.000100	0.000900

Table S9 Atomic coordinates of activated **CFA-15** (cartesian).

x	y	z	Uiso
49.167	65.508	72.731	0.026033(3000)
55.569	52.412	43.652	0.026033(3000)
18.808	30.323	43.610	0.059750(6000)
13.341	51.742	39.985	0.059750(6000)
36.990	54.055	-15.747	0.059750(6000)
44.024	35.211	-11.717	0.059750(6000)
46.187	55.209	12.975	0.045886(6000)
44.466	54.354	58.209	0.046124(6000)
26.447	36.318	-21.419	0.059750(6000)
-0.0532	36.423	37.528	0.059750(6000)
14.239	30.094	0.1005	0.059750(6000)
39.803	49.339	32.852	0.045347(6000)
0.8974	29.252	13.087	0.059750(6000)
16.211	36.558	21.715	0.059750(6000)
30.615	43.018	-10.464	0.059750(6000)
38.432	49.502	20.551	0.059750(6000)
26.982	42.028	15.096	0.059750(6000)
24.707	37.920	0.1886	0.059750(6000)
12.115	38.800	35.677	0.059750(6000)

Table S10 Bond lengths [\AA] for activated **CFA-15**.

Cu(1)-O(2)	1.89(4)	F(6)-C(6)	1.350(7)
Cu(1)-O(3)	1.890(13)	F(1)-N(1)	2.719(6)
Cu(1)-N(2)	2.083(12)	F(1)-C(5)	1.300(17)
Cu(1)-N(1)	1.963(13)	N(2)-N(1)	1.3207(15)
Cu(2)-O(3)	1.8411(12)	N(2)-C(3)	1.31(2)
Cu(2)-O(3)	1.8411(12)	O(1)-C(4)	1.2378(16)
Cu(2)-O(1)	1.936(10)	N(1)-C(1)	1.342(7)
Cu(2)-O(1)	1.936(10)	C(1)-C(2)	1.377(10)
F(2)-C(5)	1.340(15)	C(1)-C(5)	1.472(12)
F(3)-C(5)	1.369(4)	C(6)-C(3)	1.461(16)
O(2)-C(4)	1.23(4)	C(4)-C(2)	1.4722(19)
F(6)-N(2)	2.628(6)	C(2)-C(3)	1.402(9)

4. XRPD Pattern

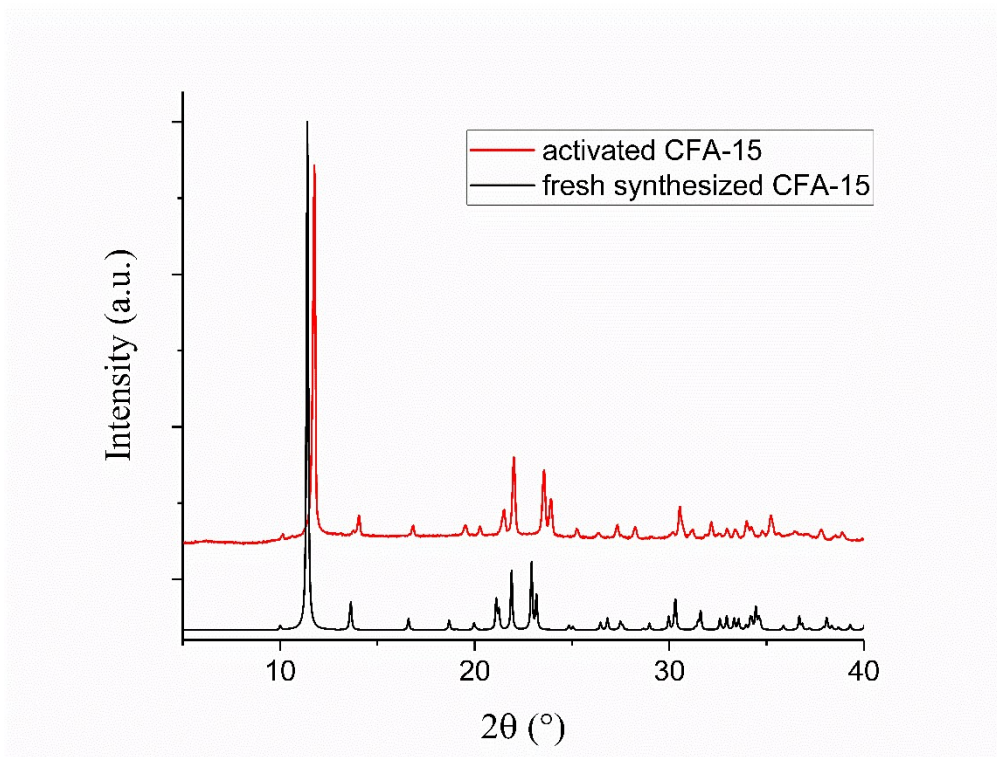


Fig. S19 X-ray powder diffraction of fresh synthesized **CFA-15** (black curve) and activated **CFA-15** (red curve).

5. Rietveld refinement plots

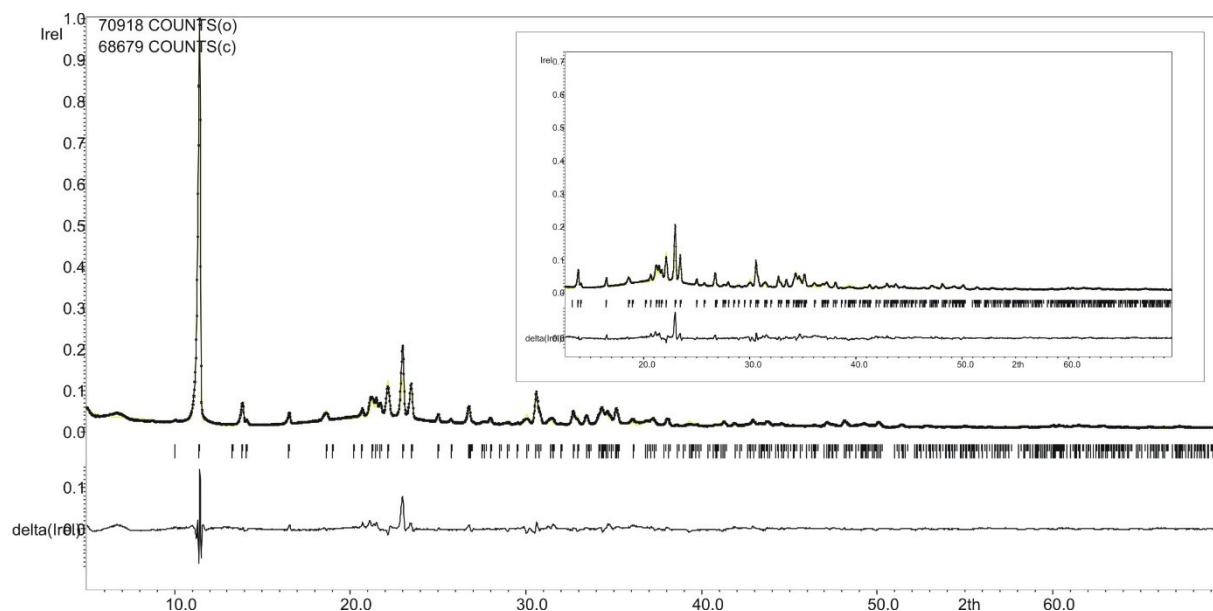


Fig. S20 Rietveld refinement plots for activated **CFA-15**. Dotted and solid lines represent observed and calculated patterns, respectively with peak markers and the difference plot shown at the bottom. XRPD data were collected at 250 °C. For clarity, the inset shows an expended view in the range 15-70° 2θ.

6. DFT Calculations

Ab initio PW-DFT-D calculations were performed on structural derivatives of **CFA-15**, where the bridging DMF linkers of the original structure have been replaced by different probe gases. All calculations were performed with the CASTEP plane-wave pseudopotential DFT code (as part of the 2019 release of BIOVIA Materials Studio). (Ref.: Clark, S. J.; Segall, M. D.; Pickard, C. J.; Hasnip, P. J.; Probert, M. J.; Refson, K.; Payne, M. C. "First principles methods using CASTEP", Zeitschrift fuer Kristallographie, 220 (5-6), 567-570 (2005)). Dispersion corrected lattice energies have been calculated for fully relaxed 3D periodic models of the primitive cells of activated **CFA-15**, and $\mu_2\text{-X}@\text{CFA-15}$ ($\mu_2\text{-X} = \text{CO}, \text{CO}_2, \text{O}_2, \text{NO}$), as well as for the neat probe gases. For all **CFA-15** derivatives spin-polarized DFT calculations were performed employing on-the-fly-generated norm-conserving plane-wave pseudopotentials with a plane wave basis set cut-off of 940 eV. In all DFT calculations the PBE gradient-corrected functional was used (Ref.: Perdew, J.P.; Burke, K.; Ernzerhof, M. "Generalized Gradient Approximation Made Simple", Phys. Rev. Lett., 77, 3865-3868 (1996)). To account for long-range noncovalent forces, such as hydrogen bonding and van der Waals (vdW) interactions, an atom-pairwise dispersion correction as introduced by Grimme was applied (Ref.: Grimme, S. "Semiempirical GGA-Type Density Functional Constructed with a Long-Range Dispersion Correction", J. Comput. Chem., 27, 1787 (2006).) Gas sorption energies were obtained from energy differences according to:

$$\Delta E^{\text{sorp}} = E^{\text{latt}}(\mu_2\text{-X}@CFA-15) - (E^{\text{latt}}(CFA-15) + E(X)),$$

with: $E^{\text{latt}}(\mu_2\text{-X}@CFA-15)$... dispersion corrected final DFT energy for the fully relaxed primitive cell of $\mu_2\text{-X}@CFA-15$;
 $E^{\text{latt}}(CFA-15)$... dispersion corrected final DFT energy for the fully relaxed primitive cell of CFA-15;
 $E(X)$...DFT energy for X (X= CO, CO₂, O₂, NO)

Table S11. Dispersion corrected DFT-D energies and energy differences for CFA-15 derivatives.

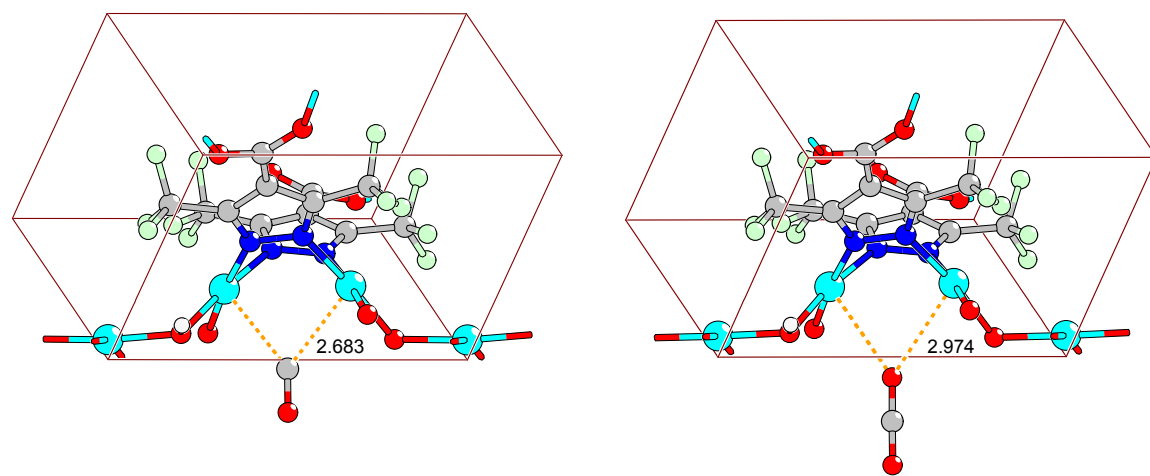
Gases (X) DFT-D energies	[eV]
CO	-584.5284096775
CO ₂	-1016.645284540
O ₂	-858.2194933184
NO	-697.4926910591

CFA-15 DFT-D energies	[eV]
CFA-15	-17031.28349762
$\mu_2\text{-CO@CFA-15}$	-17616.13847176
$\mu_2\text{-CO}_2\text{@CFA-15}$	-18048.28669126
$\mu_2\text{-O}_2\text{@CFA-15}$	-17889.67357483
$\mu_2\text{-NO@CFA-15}$	-17729.01870997

ΔE^{sorp} energies	[eV]	[kJ mol ⁻¹]
$\mu_2\text{-CO@CFA-15}$	-0.3265644	-31.5
$\mu_2\text{-CO}_2\text{@CFA-15}$	-0.3579091	-34.5
$\mu_2\text{-O}_2\text{@CFA-15}$	-0.1705838	-16.5
$\mu_2\text{-NO@CFA-15}$	-0.2425212	-23.4

Table S12. Selected crystallographic parameters for fully relaxed cells of CFA-15 derivatives (primitive representations of c-centered monoclinic cells)

Name	Formula	<i>a</i> (= <i>b</i>), <i>c</i> [Å]	α (= β), γ [°]
CFA-15	C ₁₂ H ₂ N ₄ O ₆ F ₁₂ Cu ₃	8.553766, 9.134338	103.72878, 64.91620
$\mu_2\text{-CO@CFA-15}$	C ₁₃ H ₂ N ₄ O ₇ F ₁₂ Cu ₃	8.589890, 9.254383	104.93698, 63.12424
$\mu_2\text{-CO}_2\text{@CFA-15}$	C ₁₃ H ₂ N ₄ O ₈ F ₁₂ Cu ₃	8.560388, 9.211171	104.75330, 63.13517
$\mu_2\text{-O}_2\text{@CFA-15}$	C ₁₂ H ₂ N ₄ O ₈ F ₁₂ Cu ₃	8.561768, 9.166613	104.25059, 63.01279
$\mu_2\text{-NO@CFA-15}$	C ₁₂ H ₂ N ₅ O ₇ F ₁₂ Cu ₃	8.670074, 9.266058	105.09386, 64.54344



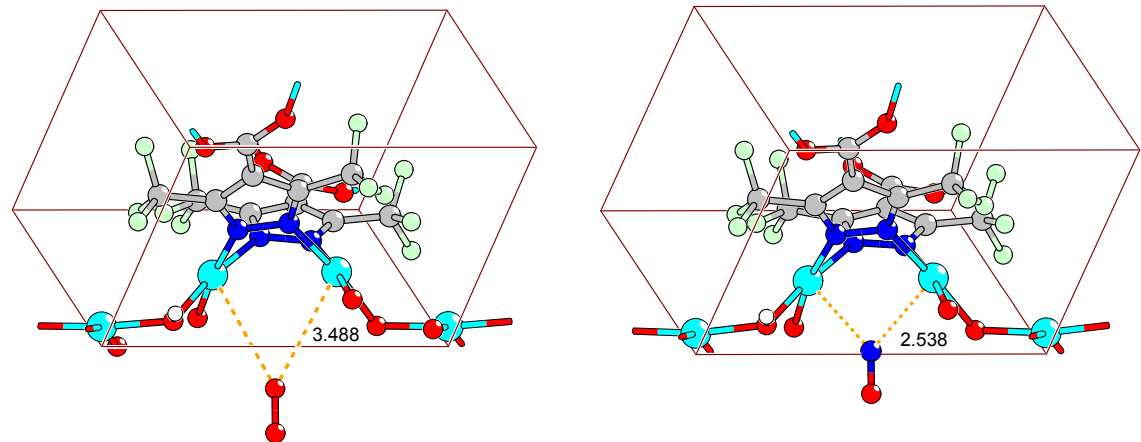


Figure S21. Primitive cells of DFT calculated μ_2 -X@CFA-15 cells showing the μ_2 -bridging coordination mode of gases X (X = CO, CO₂, O₂, NO). Selected Cu(II)---X distances [Å] are displayed within each plot. (Atom color codes: C, grey; H, white; O, red; N, blue; F, green; Cu, cyan).